Experimental Analysis of Variety of Faults in Asynchronous Squirrel Cage Motor

K. Vinoth Kumar[1], S. Suresh Kumar[2], A. Immanuel Selvakumar[3]

[1]*Department of Electrical and Electronics Engineering, School of Electrical Sciences, Karunya University, Coimbatore, India*

[2]*Department of Electronics and Communication Engineering, Dr.NGP Institute of Technology, Coimbatore, India*

[3]*Department of Electrical and Electronics Engineering, School of Electrical Sciences, Karunya University, Coimbatore, India*

kvinoth_kumar84@yahoo.in

***Abstract*— This paper deals with the diagnosis of induction motors (IM) with the so-called motor current signature analysis (MCSA). The MCSA is one of the most efficient techniques for the detection and the localization of electrical and mechanical failures, in which faults become apparent by harmonic components around the supply frequency. This paper presents a summary of the most frequent faults and its consequences on the stator current spectrum of an IM. A three-phase IM model was used for simulation taking into account in one hand the normal healthy operation and in the other hand the broken rotor bars, the shorted turns in the stator windings, the voltage unbalance between phases of supply and the abnormal behavior of load. The MCSA is used by many authors in literature for faults detection of IM. The major contribution of this work is to prove the efficiency of this diagnosis methodology to detect different faults simultaneously, in normal and abnormal functional conditions. The results illustrate good agreement between both simulated and experimental results.**

***Index Terms*— Induction motor, fault diagnosis, multiple faults, motor current signature analysis.**

I. INTRODUCTION

The Induction motors play an important role in industry for the rotating machine practice because of their hardiness low costs and quasi-absence of maintenance. Nevertheless, it arrives that this machine presents an electric or mechanical defect. The faults of these machines are varied. Seshadrinath, J. ; Singh, B et al. (2012): Interturn short circuit is often confused with voltage imbalance in induction machines. Therefore, detection and classification of single-turn fault (TF) are becoming important in the presence of voltage imbalances, under various loading conditions. Substantial studies are conducted on the interturn fault detection, but a comprehensive method for classifying the faults at different operating points of the machine, under varying supply conditions, is still a challenge. This is a critical problem in industries since the induction motors form the major workhorses. The artificial-intelligence-based techniques are advanced methods in fault monitoring. This, when combined with optimization techniques, is expected to give improved and accurate results with minimum false alarms. In this paper, a technique is developed, based on recent developments in the wavelet-based analysis, particularly in the complex wavelet domain. The support vector machines are adopted for comparing the classification accuracy obtained using complex-wavelet- and standard discrete-wavelet-based methods. Siraki, A.G. ; Gajjar, C. et.al (2012): A similar algorithm is used to extract the symmetrical components from the current and voltage signals to handle the unbalanced supply conditions. Gyftakis, K.N. ; Spyropoulos, D.V (2013): In this paper, a study of the influences of the broken bar fault to the electromagnetic characteristics of the induction motor is presented, using an asynchronous cage motor and finite element method analysis. Yang, C. ; Kang, T. (2014): Axial cooling air ducts in the rotor of large induction motors are known to produce magnetic asymmetry and can cause steady-state current or vibration spectrum analysis based fault detection techniques to fail. If the number of axial air ducts and that of poles are identical, frequency components that overlap with that of rotor faults can be produced for healthy motors. False positive rotor fault indication due to axial ducts is a common problem in the field that results in unnecessary maintenance cost. However, there is currently no known test method available for distinguishing rotor faults and false indications due to axial ducts other than offline rotor inspection or testing. Considering that there is no magnetic asymmetry under high slip conditions due to limited flux penetration into the rotor yoke, the detection of broken bars under the start-up transient is investigated in this paper. Iyer, K.L.V. ; Xiaomin Lu (2014): elucidates the significance of fault detection (FD) and voltage regulation (VR) in the aforementioned application. Chi-Man Vong (2013): Simultaneous-fault diagnosis is a common problem in many applications and well-studied for time-independent patterns. However, most practical applications are of the type of time-dependent patterns. Estima, J.O (2014): Accordingly, this paper presents a novel diagnostic algorithm that allows the real-time detection and localization of multiple power switch open-circuit faults in inverter-fed ac motor drives. Toma, S (2013): This paper deals with a new transformation and fusion of digital input patterns used

This work was supported by the Karunya University, Coimbatore

to train and test feedforward neural network for a wound-rotor three-phase induction machine windings short-circuit diagnosis. Soualhi, A et.al (2013) :The presence of electrical and mechanical faults in the induction motors (IMs) can be detected by analysis of the stator current spectrum. However, when an IM is fed by a frequency converter, the spectral analysis of stator current signal becomes difficult. For this reason, the monitoring must depend on multiple signatures in order to reduce the effect of harmonic disturbance on the motor-phase current. The aim of this paper is the description of a new approach for fault detection and diagnosis of IMs using signal-based method. It is based on signal processing and an unsupervised classification technique called the artificial ant clustering. Ben Khader Bouzid, M.et.al (2013): This paper proposes new expressions of symmetrical components (SCs) of the stator currents of the induction motor (IM) in steady state and under different stator faults, useful to ensure an efficient fault diagnosis. In this paper, the considered stator faults are interturns short circuit, phase-to-phase, and single-phase-to-ground faults. An analytical study of the behavior of these expressions shows that, under balanced supply voltage, the phase angle and the magnitude of the negative- and zero-sequence currents can be considered as reliable indicators of stator faults of the IM. Yong-Hwa Kim et.al (2013): The classical multiple signal classification (MUSIC) method has been widely used in induction machine fault detection and diagnosis. This method can extract meaningful frequencies but cannot give accurate amplitude information of fault harmonics. In this paper, we propose a new frequency analysis of stator current to estimate fault-sensitive frequencies and their amplitudes for broken rotor bars (BRBs). The proposed method employs a frequency estimator, an amplitude estimator, and a fault decision module. The frequency estimator is implemented by a zoom technique and a high-resolution analysis technique known as the estimation of signal parameters via rotational invariance techniques, which can extract frequencies accurately. For the amplitude estimator, a least squares estimator is derived to obtain amplitudes of fault harmonics, without frequency leakage. In the fault decision module, the fault diagnosis index from the amplitude estimator is used depending on the load conditions of the induction motors. The fault index and corresponding threshold are optimized by using the false alarm and detection probabilities. However the most frequent are (Benbouzid (2000), Razik (2002) and Trajin et al. (2008): opening or shorting of one or more of a stator phase winding, broken rotor bar or cracked rotor end rings, static or dynamic air-gap irregularities, and bearing failures. In order to avoid such problems, these faults have to be detected to prevent a major failure from occurring. It is well known that a motor failure may yield an unexpected interruption at the industrial plant, with consequences in costs, product quality, and safety. During the past twenty years, there has been a substantial amount of fundamental research into the creation of condition monitoring and diagnostic techniques for IM drives. Different detection approaches proposed in the literature, those based on the Extended Park's Vector Approach (EPVA), which allows the detection of inter-turn short circuits in the stator winding (Acosta et al. (2004)). The EPVA is appropriate for the stator windings monitoring. Çalis and Çakir (2007) used th e $2.s.f_s$ spectral component in the stator current zero crossing times (ZCT) spectrum as an index of rotor bar faults. However, the major deficiency for this fault indicator, for low slip IM Operating at no load condition it may then be difficult to read its value. In Casimir et al. (2006), the authors studied the diagnosis of IM by pattern recognition method. This method consists in extracting features from the combination of the stator currents and voltages. Some of these features could be irrelevant or redundant. Therefore, the Sequential Backward Selection (SBS) algorithm is applied to the complete set of features to select the most relevant. Then they used the k-Nearest Neighbours (kNN) rules to monitor the IM functioning states. This rule is applied with reject options in order to avoid automatic classifications and diagnosis errors. Didier et al. (2007) employed the Fourier Transform of the stator current and they analyzed its phase. It is shown that the basically calculated phase gives good results when the motor operates near its nominal load. For weak load, the results obtained are not robust enough for the detection of an incipient rotor fault. In Li and Mechefske (2004), the authors used the vibration monitoring methodology to detect incipient failures in IM. Vibration monitoring system requires storing of a large amount of data. Vibration is often measured with multiple sensors mounted on different parts of the machine. The examination of data can be tedious and sensitive to errors. Also, fault related machine vibration is usually corrupted with structural machine vibration and noise from interfering machinery. To overcome these problems Poyhonen et al. (2003) used the Independent Component Analysis (ICA) to compress measurements from several channels into a smaller amount of channel combinations and to provide a robust and reliable fault diagnostics routine for a cage IM. This paper is focused on the Motor Current Signature Analysis (MCSA) approach. This technique utilizes results of spectral analysis of the stator current (precisely, the supply current) of an IM to spot an existing or incipient failure of the motor or the drive system. It is claimed that MCSA monitoring is the most reliable method of assessing the overall health of a rotor system (Thomson (2001)). Unlike the greater part of techniques, MCSA can provide the same indications without requiring access to the motor.

II. DIFFERENT TYPES OF FAULTS

A. Broken Rotor Bars

It is well known that, under normal conditions of working, a 3-phase IM with symmetrical stator winding fed from a symmetrical supply voltage with frequency f_S, will produce a resultant forward rotating magnetic field at synchronous speed and if exact symmetry exists there will be no resultant backward rotating field. When rotor defect appears, it creates in addition of the direct rotor field an inverse field that turns to the speed ($-s.\omega_s$). It is due to the fact that the rotor currents are now direct and inverse following the unbalance of resistances. It is the interaction of this field with the one descended of stator windings that induces an e.m.f. and current in the stator winding at (1-

2.s).f_s. This cyclic current variation causes a speed oscillation at twice the slip frequency (2.s.f_s) and finally, this speed oscillation induces, in the stator current spectrum, an upper component at (1+2.s).f_s, and so on (Çalis and Çakir (2007) and Mehala and Dahiya (2009)). Therefore, broken rotor bars induce harmonic components in the stator current at frequencies given by (Thomson (2009) and Jung et al. (2006)):

$$f_{bb} = (1 \pm 2.k.s) f_s \quad (1)$$

Where: k = 1, 2, 3…, $\kappa \in \mathbb{N}$, f_{bb} : broken rotor bar frequency, f_s : electrical supply frequency, p : number of pole pairs,

s : slip.

B. Unbalanced Supply Voltage

Asymmetrical stator faults (caused by stator winding faults or asymmetrical supply voltages) are also common in IM (Messaoudi et al. (2007)). An asymmetrical stator supply voltage can be caused by the opening of one of the three phases, by the presence of one-phase-load in the environment near of the motor, or by the source. The consequences of an unbalanced supply voltage applied to a three phase IM are the reduction of the useful torque and the increase of the losses. Unbalances result in an inverse component that generates high rotor current provoking a very important heating of the rotor and implying an overheating of the motor. The calculation of the unbalance can be approached by the following equation:

$$\text{unbalance } (\%) = 100 \times Max\left(\frac{V_h - V_{av}}{V_{av}}, \frac{V_{av} - V_l}{V_{av}}\right) \quad (2)$$

Where:

V_h : highest voltage,

V_l : lowest voltage,

$$V_{av} = (V_1 + V_2 + V_3)/3 \quad (3)$$

An unbalanced in the supply voltage induces sidebands in stator current spectrum of the IM at the following frequencies:

$$f_{usv} = (1 + 2.k) f_s \quad (4)$$

Where: k = 1, 2, 3…, $\kappa \in \mathbb{N}$,

f_{usv} : unbalanced supply voltage frequency, f_s : electrical supply frequency.

C. Fluctuation in Load Torque

The load torque variation induces components in the current spectrum which coincide with those caused by a fault condition. In an ideal machine where the stator flux linkage is purely sinusoidal, any oscillation in the load torque at a multiple of the rotational speed will produce stator currents at frequencies of (Benbouzid (2000) and Fenger et al. (2003)):

$$f_{lo} = f_s \pm k.f_r = \left[1 \pm k\left(\frac{1-s}{p}\right)\right] f_s \quad (5)$$

Where: k = 1, 2, 3…, $\kappa \in \mathbb{N}$, f_{bb}

f_{lo} : load effects frequency,

f_s : electrical supply frequency,

f_r : mechanical rotor speed in Hertz, p : number of pole pairs,

s : slip.

D. Shorted Turns in Stator

Asymmetrical Inter-turn short circuits in stator windings constitute a category of faults that is most common in induction motors. Typically, short circuits in stator windings occur between turns of one phase, or between turns of two phases, or between turns of all phases. Moreover, short circuits between winding conductors and the stator core also occur. Studies in (Thomson (2001) and Blodt et al. (2006)) prove that the stator current is enriched by short turns. The additional components are at the following frequencies:

$$f_{st} = \left[\frac{n}{p}(1 - s) \pm k\right] f_s \quad (6)$$

Where: k = 1, 2, 3…, $\kappa \in \mathbb{N}$, f_{bb}

f_{st} : short turns frequency,

f_s : electrical supply frequency,

p : number of pole pairs,

s : slip.

III. Simulation And Experimental Results

2.1Motor Test Ring

The Experimental setup shown in Fig 1 is also instrumented with Hall-effect current transducers. The motor current spectrum analysis algorithm is implemented using MATLAB software package. The acquisition of stator current takes place at a sampling frequency of 10 kHz on a length of 10 seconds.

The experimental setup consists of two IMs; the first one is a 0.375 kW, 4-poles, 22-rotor bars IM. Fig 2 shows how damage in one of the rotor bars was physically seeded. It was performed by drilling through one of the aluminium conductors that made up the squirrel cage. The second motor used is a 3 kW IM, in witch, two extra outputs are created as shown in Fig. 3. These added outputs represent respectively, the extremities of a stator phase with 5 and 8 short-circuited-windings. The load is a DC motor acted as a generator and its power output was dissipated in a variable resistor bank.

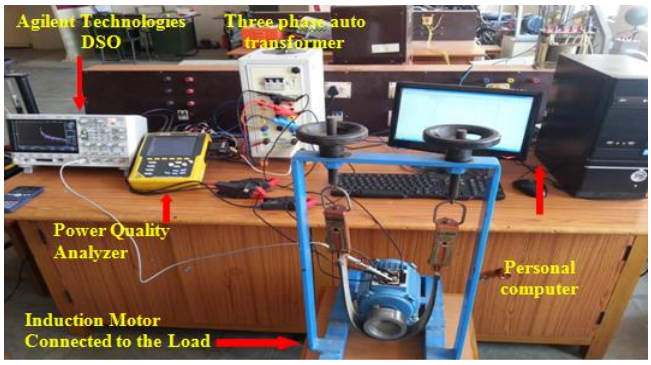

Figure 1: Experimental setup

Fig.2 Seeded broken rotor bar fault.

Fig.3. Seeded short-circuited windings in one stator phase.

B. Case Study 1: Broken Rotor Bars

Rotor fault is simulated by adding extra resistance to the single phase resistance of rotor circuit (Çalis and Çakir (2007), Didier and Razik (2001) and Treetrong (2010)). In Fig. 4, spectrum of stator current under 75% operational load is given, respectively, for healthy motor, rotor resistance increased 20% of its rated value, and rotor resistance increased 40% of its rated value. Referring to the healthy motor spectrum given by Fig. 4 (a), we can remark the apparition of sidebands around the fundamental frequency in Fig. 4 (b) and (c). These sidebands are the results of the defect created in the rotor. Frequencies of these sidebands correspond precisely to the mathematical relation $(1\pm2.s).f_s$ given by (1). The amplitude and the number of the sidebands frequencies components are proportional to the amount of broken rotor bars. Table 1, shows the harmonic components of the stator current under 75% of rated load with two levels of rotor asymmetry.

TABLE 1.
Harmonic Components of the Stator Current

Frequencies	$R_{ra}= R_r + 20\% R_r$	$R_{ra}= R_r + 40\% R_r$
$(1 - 6.s).f_s$		44,75 Hz
$(1 - 4.s).f_s$	46,70 Hz	46,50 Hz
$(1 - 2.s).f_s$	48,35 Hz	48,25 Hz
$(1 + 2.s).f_s$	51,65 Hz	51,75 Hz
$(1 + 4.s).f_s$	53,30 Hz	53,50 Hz
$(1 + 6.s).f_s$		55,25 Hz

When the IM operates with no load Fig. 5 (a), the algorithm of detection does not give any response. This means that the jump located at the frequency $(1\pm2.k.s).f_S$ is not detectable due to its low amplitude. The current which crosses the rotor bars is not important enough to create a consequent jump at this frequency.

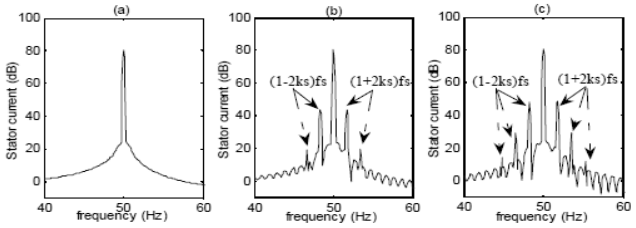

Fig. 4. Stator current spectrum under 75% operational load:

(a) healthy motor, (b) $R_{ra}= R_r + 20\% R_r$, (c) $R_{ra}= R_r + 40\% R_r$.

For an IM with a constant number of broken rotor bars operated under different levels of operational load, it is clearly seen in Fig. 5 that the amplitudes of the sidebands around the supply frequency increase as the load torque rises. Thus, this indicator component is sensitive to the load variation. Therefore, it is not exactly reflecting the fault degree. But, the amplitude of the sidebands can be used as an efficient indicator of faults degree if the load effect is taken into account. The frequencies of the first two sidebands around the fundamental frequency for an IM operating with a fixed number of broken rotor bars under 25% of its rated load are 48.81 Hz and 51.19 Hz. Figure 6 illustrates the stator current spectrum when one broken rotor bar fault was experimentally seeded. When, the motor is under 25% of its rated load as shown in Fig. 6 (a), the amplitude jump at frequencies $(1\pm2.k.s).f_S$ due to rotor fault appeared in the stator current spectrum. Despite, the fault existence (one broken rotor bar), the MCSA failed to give a positive result in the case of unloaded motor Fig. 6 (b).

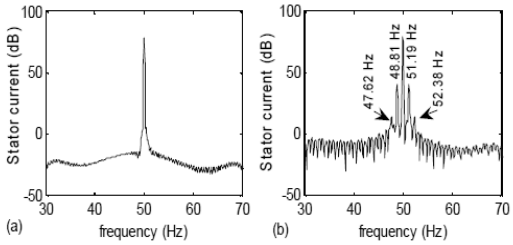

Fig. 5. Stator current spectrum with $R_{ra} = R_r + 40\% R_r$: (a) with zero load condition, (b) with 25% load condition

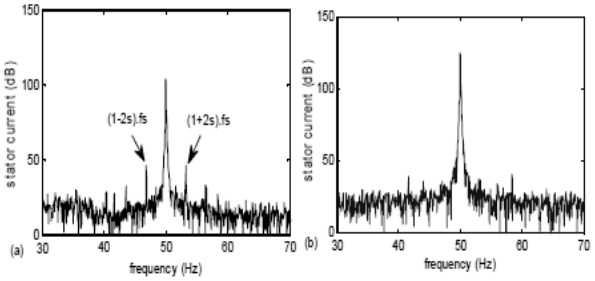

Fig. 6. Experimental stator current spectrum of an IM with broken rotor bar: (a) under 25% of load, (b) unloaded motor.

C. Case Study 2: Broken Rotor Bars and Unbalanced Supply Voltage

In order to simulate unbalanced supply faults, a V_0 drop in one phase was created. Hence the stator supply voltage equations were changes as follows:

$$V_{as}(t) = \sqrt{2}(V - V_0)\cos(\omega t),$$
$$V_{bs}(t) = \sqrt{2}V\cos\left(\omega t - \frac{2\pi}{3}\right),$$
$$V_{cs}(t) = \sqrt{2}V\cos\left(\omega t + \frac{2\pi}{3}\right). \quad (7)$$

In Fig. 7 (a), new components at frequencies $(1+2k).f_S$: (150 Hz; 250 Hz) emerge in the current spectrum. These harmonic components are induced by the unbalance in the supply voltage. Figure 7 (b) and (c), clearly, show that symptoms of both unbalanced stator voltage supply $(1+2.k).f_S$ and broken rotor bars $(1\pm2.k.s).f_S$ appear in the stator current spectrum.

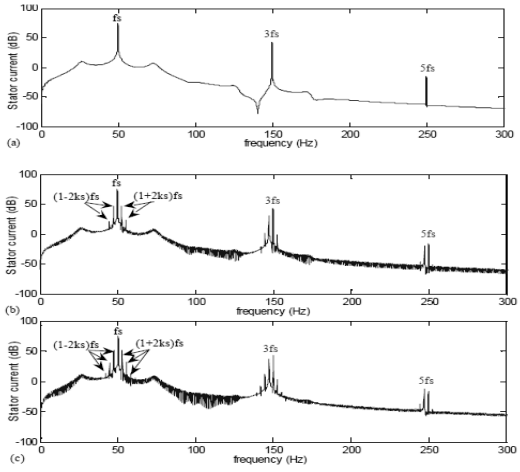

Fig. 7. Stator current spectrum for 20V drop of one phase voltage: (a) healthy rotor; (b) broken rotor bars (R_{ar}= R_r + 20% R_r); (c) broken rotor bars (R_{ar} = R_r + 40% R_r).

Figure 8 (a) and (b) illustrate the experimental results of the stator current spectrum when the IM is operated under different levels of unbalanced supply voltage. It appears in Fig. 8 (a) and Fig. 8 (b), sidebands at frequencies $(1+2k).fs$. It is clear seen that the magnitudes of these sidebands rise when the drop in the supply voltage is increased. The rise in the magnitude of sidebands created by the unbalanced supply voltage is clearer at the supply frequency third harmonic (150 Hz).

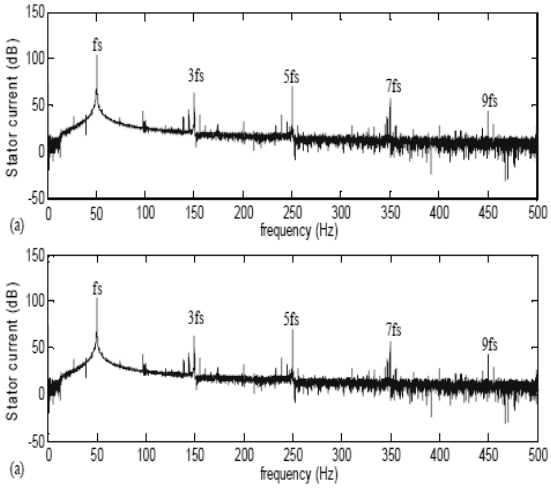

Fig. 8. Experimental stator current spectrum of IM operating under unbalanced supply voltage: (a) Partial unbalance (20 % drop in one supply voltage phase); (b) Full unbalance (opening of one phase).

D.Case Study 3: Broken Rotor Bar, Unbalanced Supply Voltage and Load Torque Fluctuation

In this section, to show the behavior of the motor operating under variable load condition, constant motor load used in the model is replaced with sinusoidal changing load as shown in (8).

$$T_l(t) = 10 + 1 \,.\, \sin(154,48\, t) \quad (8)$$

The load amplitude is equal to the rated load and the load frequency is chosen as the assumption in section (2.3). Current spectrum is given in Fig. 8. It is shown that the load variation produces sidebands around the supply frequency equal to frequencies of ($f_S \pm k.f_r$). Figure 9 depicts the current spectrum of an IM operating under three different operational conditions. In Fig. 9 (a), only the frequencies due to load variations appeared in the stator current spectrum. In Fig. 9 (b), in addition of the frequencies components due to load variations, it appeared also sidebands around the fundamental at frequencies $(1\pm2.k.s).f_s$ produced by the rotor asymmetry. In Fig. 9 (c), frequencies due to load variation, rotor asymmetry and unbalanced supply voltage appeared simultaneously in the stator current spectrum and also fig.10 shows Stator current spectrum for motor operating under variable load condition in Agilent DSOX-2014A with broken rotor bars

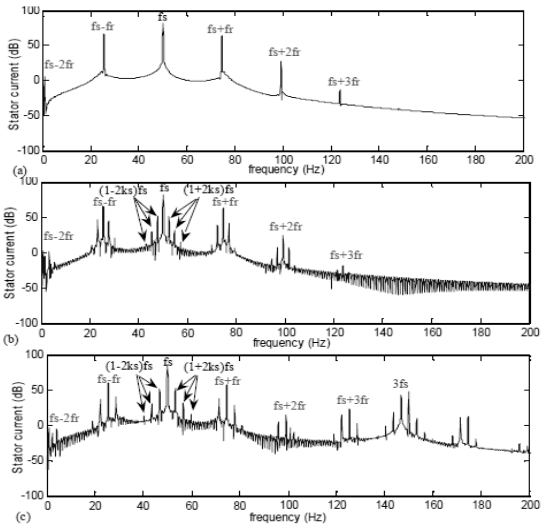

Fig. 9. Stator current spectrum for motor operating under variable load condition: (a) healthy motor; (b) motor with broken rotor bars (R_{ar}= R_r +40% R_r); (c) motor with broken rotor bars (R_{ar} = R_r +40% R_r) and 44 V drop in one phase of the supply voltage.

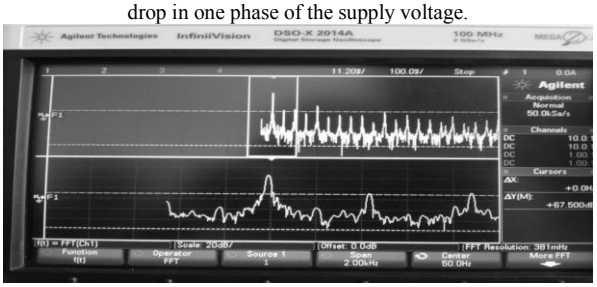

Fig. 10. Stator current spectrum for motor operating under variable load condition in Agilent DSOX-2014A with broken rotor bars

E. Case Study 4: asymmetric stator winding

Figure 11 depicts the stator current spectrum of the squirrel cage IM operating under asymmetric stator winding (5 short-circuited windings in one phase). The harmonic components due to the asymmetric stator winding appear in the stator current spectrum, despite the absence of the mechanical load.

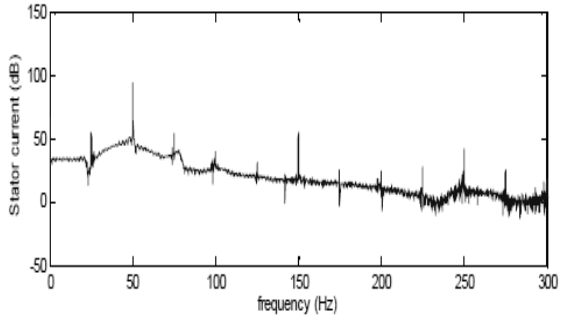

Fig. 11. Experimental stator current spectrum of unloaded IM, operating under asymmetric stator winding (5 short-circuited-windings in one phase).

Looking to all given figures, we can remark the efficiency of the MCSA method to detect different faults in the IM and to discriminate between them. Hence, this classical approach has some important advantages such as the simplicity of the data acquisition systems and the required software, along with the robustness of the tool, which has hitherto provided quite satisfactory results. Also, from the stator current spectrum analysis it is possible to detect rotor as well as stator faults. However, its validity has some drawbacks when the approach is applied under certain conditions. This is the case, for instance, of light-loaded or unloaded machines. In those situations, the slip *s* is very low and the sideband components practically overlap the supply frequency. This makes difficult to detect their presence and to use them for the diagnosis, as Didier et al. (2007) remarked. Also, the frequency characterising the fault must be computed considering the motor poles number, the slip, and the motor features in some cases. Also, another handicap of this approach is that it is not possible to relate the fault severity with the amplitude of these frequencies characterizing the fault because the amplitude depends on many factors such as the external load and the measurement noise.

IV. CONCLUSION

A review of the most frequent IM failures and their detections via the MCSA is presented. Initially, the phenomenon of asymmetrical rotor is presented and all the characteristic frequencies occurring in the stator current of IM due to cracked or broken bars are explained. Similarly, the phenomena of shorted turns in the stator windings, unbalanced stator voltage and load variation, in healthy motor and in the case of broken rotor bars, are studied. Experiment and simulation results showed the efficiency of the proposed method to Spot and discriminate between the different faults but the major drawback of this method, is in the case of light-loaded or unloaded machines it is difficult to detect faults and fortunately an IM operates most the time under its rated load torque.

REFERENCES

[1] Seshadrinath, J. ; Singh, B. ; Panigrahi, B.K. Single-Turn Fault Detection in Induction Machine Using Complex-Wavelet-Based Method, *IEEE Transactions on Industrial Applications*, vol. 48, No.6, pp. 1846-1854, 2012.

[2] Siraki, A.G. ; Gajjar, C. Khan, M.A, Barendse, Pillay, P. An Algorithm for Nonintrusive In Situ Efficiency Estimation of Induction Machines Operating With Unbalanced Supply Conditions, *IEEE Transactions on Industrial Applications*, vol. 48, No.6, pp. 1890-1900, 2012.

[3] Gyftakis, K.N. A Novel Approach for Broken Bar Fault Diagnosis in Induction Motors Through Torque Monitoring, *IEEE Transactions on Energy Conversion*, vol. 28, No.2, pp. 267-277, 2013.

[4] Yang, C. ; Kang, T. ; Hyun, D, Lee, S.B. Reliable Detection of Induction Motor Rotor Faults Under the Rotor Axial Air Duct Influence, *IEEE Transactions on Industrial Applications*, vol. 50, No.4, pp. 2493-2502, 2014.

[5] K.L.V. Iyer, Xiaomin Lu, Y. Usama, V. Ramakrishnan, N.C. Kar. A Twofold Daubechies-Wavelet-Based Module for Fault Detection and Voltage Regulation in SEIGs for Distributed Wind Power Generation, *IEEE Transactions on Industrial Electronics*, vol. 60, no. 4, pp. 1638-1651 , Apr 2013.

[6] Chi-Man Vong, Pak-Kin Wong, Weng-Fai Ip. A New Framework of Simultaneous-Fault Diagnosis Using Pairwise Probabilistic Multi-Label Classification for Time-Dependent Patterns, *IEEE Transactions on Industrial Electronics*, vol. 60, no. 8, pp. 3372-3385 , Aug 2013.

[7] J.O. Estima, A.J. Marques Cardoso. A New Algorithm for Real-Time Multiple Open-Circuit Fault Diagnosis in Voltage-Fed PWM Motor Drives by the Reference Current Errors, *IEEE Transactions on Industrial Electronics*, vol. 60, no. 8, pp. 3496-3505 , Aug 2013.

[8] S. Toma, L. Capocchi, G.-A. Capolino. Wound-Rotor Induction Generator Inter-Turn Short-Circuits Diagnosis Using a New Digital Neural Network, *IEEE Transactions on Industrial Electronics*, vol. 60, no. 9, pp. 4043-4052 , Sep 2013.

[9] A. Soualhi, G. Clerc, H. Razik. Detection and Diagnosis of Faults in Induction Motor Using an Improved Artificial Ant Clustering Technique, *IEEE Transactions on Industrial Electronics*, vol. 60, no. 9, pp. 4053-4062 , Sep 2013.

[10] M. Ben Khader Bouzid, G. Champenois. New Expressions of Symmetrical Components of the Induction Motor Under Stator Faults, *IEEE Transactions on Industrial Electronics*, vol. 60, no. 9, pp. 4093-4102 , Sep 2013.

[11] Yong-Hwa Kim, Young-Woo Youn, Don-Ha Hwang, Jong-Ho Sun, Dong-Sik Kang. High-Resolution Parameter Estimation Method to Identify Broken Rotor Bar Faults in Induction Motors, *IEEE Transactions on Industrial Electronics*, vol. 60, no. 9, pp. 4103-4117 , Sep 2013.

[12] Acosta, G.G., Verucchi, C.J., and Gelso, E.R. A current monitoring system for diagnosing electrical failures in induction motors. *Mechanical Systems and Signal Processing*, vol. 20, pp. 953-965, 2004.

[13] Benbouzid, M.E.H. A Review of induction motors signature analysis as a medium for faults detection. *IEEE Transactions on Industrial Electronics*, vol. 47, no. 5, pp. 984-993,2000.

[14] Blodt, M., Chabert, M., Regnier, J., Faucher, J. Mechanical Load Fault Detection in Induction Motors by Stator Current Time-Frequency Analysis. *IEEE Transaction on Industry Applications*, vol. 42, n. 6, pp. 1454–1463,2006.

[15] Casimir, R., Boutleux, E., Clerc, G., and Yahoui, A. The use of features selection and nearest neighbours rule for faults diagnostic in induction motors. *Engineering Applications of Artificial Intelligence*, vol. 19, pp. 169-177,2006

[16] Çalis, H., and Çakir, A. Rotor bar fault di agnosis in three phase induction motors by monitoring fluctuations of motor current zero crossing instants. *Electric Power System Research*, vol. 77, no. 5-6, pp. 385-392,2007.

[17] Didier, G., Ternisien, E., Caspary, O., and Razik, H. A new approach to detect broken rotor bars in induction machines by current spectrum analysis. *Mechanical Systems and Signal Processing*, vol. 21, no. 2, pp. 1127-1142,2007.

[18] Didier, G., and Razik, H. Sur la détection d'un défaut au rotor des moteurs asynchrones. *3EI magazine*, no. 27, pp. 53-62, 2001.